Highly functional lactic acid ring-opened soybean polyols applied to rigid polyurethane foams

Rodrigo Herrán,[1] Javier Ignacio Amalvy,[1] Leonel Matías Chiacchiarelli [2,3]

[1]Instituto de Investigaciones Fisicoquímicas Teóricas y Aplicadas, CCT La Plata CONICET-UNLP, Diagonal 113 y 64, La Plata, Argentina

[2]Instituto de Tecnología de Polímeros y Nanotecnología, CONICET-UBA, Avenida General Las Heras 2214, Buenos Aires, Argentina

[3]Departamento de Ingeniería Mecánica, Instituto Tecnológico de Buenos Aires, Avenida Eduardo Madero 399, Buenos Aires, Argentina

Correspondence to: L. M. Chiacchiarelli (E-mail: lmchiacchiarelli@yahoo.com.ar)

ABSTRACT: We synthesized polyols with high hydroxyl functionalities (F_{OH}s), between 9.0 and 12.6, and characterized them with differential scanning calorimetry, thermogravimetric analysis, and size exclusion chromatography after we parametrically studied the ring-opening reaction of epoxidized soybean oil with lactic acid (LA) as a function of the reaction temperature and lactic acid equivalent frac-tion (f_{LA}). An increase of only 20°C in the reaction temperature (from 80 to 100°C) caused changes in the hydroxyl number (+17.8%), F_{OH} (−25%), viscosity (−14.0%), and oligomeric content (−24.1%). f_{LA} mostly affected the ring-opening yield, and only for f_{LA} values above 0.4 was possible to achieve values higher than 80%. Rigid polyurethane foams (rPUFs) were synthesized and characterized with scanning electron microscopy, dynamic mechanical analysis (DMA), and compressive mechanical tests. rPUFs with a very high specific compres-sive strength (7.8 kPa kg^{-1} m^3) were synthesized solely with biobased soybean oil. DMA revealed a compromised relationship between the specific compressive strength and its temperature dependence. To increase the first one, the most relevant method was to increase F_{OH}. Instead, to increase the latter one, the OH number had to be maximized.

KEYWORDS: biopolymers and renewable polymers; biosynthesis of polymers; mechanical properties; polyurethane

Received 9 November 2018; accepted 23 April 2019

INTRODUCTION

Over the past decades, the production of polymers from carbon-neutral resources has gained especial attention in contrast to polymers synthesized from nonrenewable resources.[1–6] The main reasons associated with this transition are the continuous depletion of fossil fuels and environmental sustainability. Nowadays, a variety of chemicals are obtained from vegetable oils, polysaccharides, wood, and proteins.[7,8] Among these, vegetable oils represent a promising route toward the synthesis of several chemical precursors. They are considered to be one of the cheapest and most abundant biological resources and to have the advantage of inherent biodegradability and reduced toxicity. Vegetable oils are currently being used for the synthesis of both thermoplastic and thermosetting polymers.[9–14] To achieve this, it is important to functionalize the triglyceride molecule. For example, an epoxy functionality can be obtained on the C═C double bonds of a soybean oil through reactions with peroxoacetic and peroxoformic acids.[15]

Polyurethanes are one of the most versatile polymers because isocyanates react with several chemical groups; this provides a way to obtain a full spectrum of applications, such as adhesives,[16] insulation foams,[17–22] coatings,[23] and biomedical devices.[24] Rigid polyurethane foams (rPUFs) represent a material of choice for improving the energy efficiency of buildings. However, rPUFs are synthesized mainly from polyols and polyisocyanates (in the presence of additives and catalysts), which are obtained from nonrenewable resources. Such an approach affects the sustainability of the construction industry.[25] Recently, the replacement of these precursors by nontoxic and renewable ones has become a universal objective for preventing environmental issues and attaining sustainability. Until now, the production of polyols from natural resources has been more successful than that that from isocyanates, and several production paths are currently used as alternatives in industry. Among polyols used for the synthesis of polyurethanes, it is known that polyesters represent an expensive but high-performance alternative with respect to polyether polyols.[26,27] In addition, its synthetic path uses highly toxic catalysts (organometallic), and it has a low yield. Then, it becomes imperative to obtain biobased polyesters from synthetic paths that do not use highly toxic catalysts. Several vegetable oils can be used to achieve this objective, soybean oil

being one of the most promising candidates,[28,29] especially in developing countries such as Argentina and Brazil. High-value polymers produced from renewable raw materials could have a profound impact on the economies of such developed countries. However, one of the main drawbacks of soybean oil compared to other biobased polyols, such as castor oil,[17,29] is that it does not contain a hydroxyl functionality (F_{OH}). As proposed by Chiacchiarelli and coworkers,[17,29] the use of nanoparticles might be useful for alleviating such an issue; however, it is also important to seek alternative synthesis conditions to obtain soybean polyols with high F_{OH}s.

Several pathways for synthesizing polyols from soybean oil have been studied,[1,2,30–34] for instance, thiol–ene reactions,[35] hydrogenation,[36] ozonolysis,[37] hydroformylation,[38] transesterification,[39] and the ring opening of epoxidized oils.[40] The last consists of a two-step procedure in which, first, the double bond of the triglycerides are epoxidized and, second, oxirane rings formed are opened by a so-called ring-opening agent (ROA). A wide range of agents have been used for this purpose. Among those, the use of lactic acid (LA) as an ROA is one of the most promising routes because it is obtained by the fermentation of renewable raw materials, such as corn, potato, and other agricultural products.[41] Another relevant reason is that an ROA based on LA can lead to polyols with higher functionalities, a key aspect for the synthesis of rPUFs. However, until now, the maximum F_{OH} obtained in the literature ranged up to 4.0.[42–44] Miao *et al.*[42] studied the synthesis of high-glass-transition-temperature (high-T_g) polyurethanes after the ring-opening reaction (ROR) of epoxidized soybean oil (ESO). Even though the objective was achieved, the role of the oligomeric species after the ROR step on the properties of the polyol was not reported. On the other hand, Caillol *et al.*[43] found that the oligomeric content of such a reaction was 44 wt %. However, the dependence of the oligomeric content on the reaction parameters and its effect on the polyol properties was not studied. In addition, the thermal transitions of such polymeric species were only studied by Li and Sun.[44] From these studies, we inferred that even though biobased polyols were synthesized from soy oil, the fact that the maximum achieved F_{OH} ranged around 4.0 would prevent its successful application as a polyol for rPUFs. In fact, in some studies, rPUFs have been formulated with glycerol because the functionality of the original soybean polyol was not high enough to obtain a considerable T_g and crosslinking density.

In this study, we focused on the ROR of an ESO to obtain biobased polyester polyols from a green, nontoxic method. In contrast to previous studies, we focused on the effects of the reaction temperature and lactic acid equivalent fraction (f_{LA}) on the yield of the ROR and the oligomeric content of the resulting reaction species with size exclusion chromatography (SEC). Fourier transform infrared (FTIR) analysis was performed to evaluate how the oxirane group evolved as a function of the ROR conditions. The thermal transitions, viscosity, and thermal degradation of the resulting polymer were studied with differential scanning calorimetry (DSC), viscometry, and thermogravimetric analysis (TGA) techniques. In addition, the rPUFs were synthesized solely with ESO–LA without additional crosslinkers and characterized with scanning electron microscopy, compression mechanical tests, and dynamic mechanical analysis (DMA).

EXPERIMENTAL

Soybean-based polyols were synthesized from ESO (commercial name KALFLEX 13, Varteco) with 98% purity and an oxirane oxygen content of 6.75%. LA (90%) was obtained from Parafarm. Sodium chloride and EtOAc (Cicarelli, ACS) were used in the purification stage. Concentrated hydrochloric acid (American Chemical Society [ACS] grade) was purchased from Quimicor. Bromophenol blue indicator and di-isobutyl amine (ACS) were purchased from Stanton. A polymeric diphenylmethane diisocyanate (Suprasec 5005, Huntsman) was used as the isocyanate component (Figure 1). Before each experiment, the isocyanate index was corroborated by means of HCl backward titration according to the guidelines from ASTM D 2572. As recommended by this standard, the titration procedure was performed over three samples of 0.1 g of isocyanate. A polysiloxane-based silicone was used as the surfactant (Niax L585). The blowing agent (BA) was distilled water.

The rPUFs were prepared by the one-shot method,[26] whereas all of the components except the isocyanate were dispersed with a homogenizer (MyV mixer) at 4000 rpm for 4 min. Before each experiment, the biobased polyol was degassed at 30 mbar under stirring with a cowles stirrer at 4000 rpm. Then, the polyol and the isocyanate were introduced in a High Density Poliethylene cylindrical mold with an internal diameter of 70 mm and rapidly dispersed with a cowles stirrer rotating at 2500 rpm for 30′. A K-type thermocouple coupled with an ultrasonic distance sensor (HC-sr05) were used to take *in situ* measurements of the temperature and foam growth distance. For each specimen, cubic samples with sides of approximately 25 mm were cut with a computer-controlled band saw. Finally, the samples were weighed (Ohaus Adventurer) and accurately measured to obtain the apparent density. Quasi-static compressive experiments were tested with a universal testing machine (Instron 5535) with a 20kN load cell and a crosshead speed of 2.5 mm/min.

The reaction between ESO and LA (Figure 1) was carried out in a 250 mL, three-necked, round-bottom flask, and the reactants mass was weighed to the nearest 0.1 mg to reach a final volume of 35 mL. The blend was mechanically stirred in the presence of nitrogen (purity = 99.998%) for 15 min, and later, the flask was immersed in a heating bath for 5 h under isothermal conditions. Once the reaction ended, 100 mL of EtOAc was added to the flask, and the LA excess was removed with a saturated aqueous solution of sodium chloride until a neutral pH was attained. Finally, the solvent was removed *in vacuo*, and we obtained a viscous yellow oil, which was dried at 60°C for 2 h *in vacuo*.

f_{LA} values between 0 and 0.5 were used (viz., 0, 0.15, 0.28, 0.33, 0.4, and 0.5); these were calculated via the assumption that LA was monovalent,[42] as follows:

$$f_{LA} = \frac{e_{LA}}{e_{total}} = \frac{e_{LA}}{e_{LA} + e_{oxirane}} \quad (1)$$

where e_x is the number of equivalents of each species.

The ROR reaction of ESO was performed in the range 80–100°C. The lower temperature value was selected on the basis of the reaction enthalpy obtained from DSC experiments (TA Q200). By performing a dynamic temperature ramp at 2°C/min, we

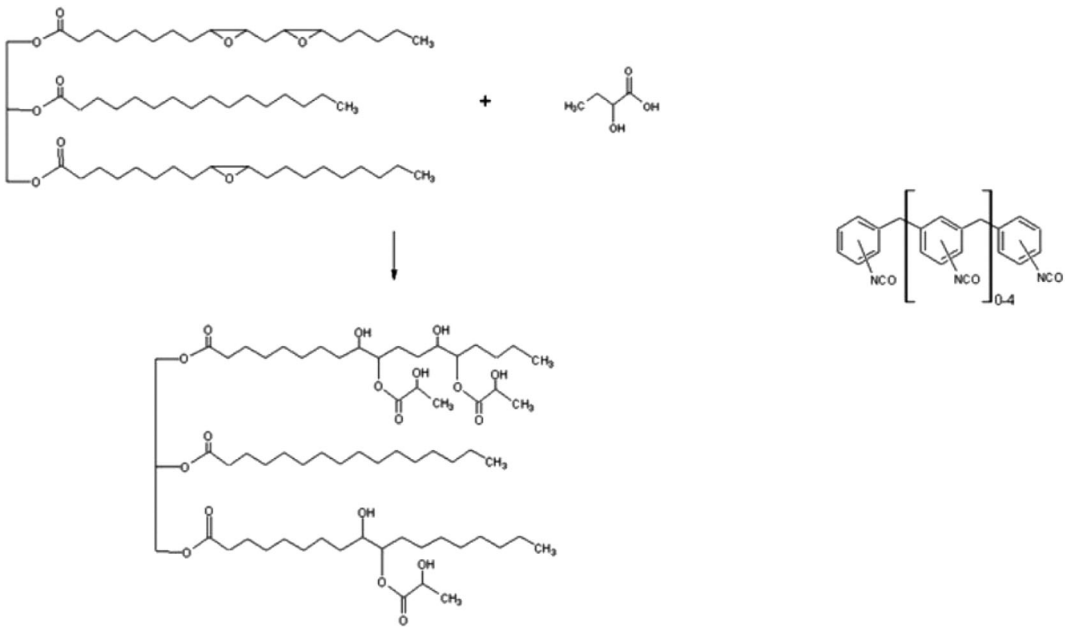

Figure 1. Schematic of the diisocyanate used in this study and the ROR between ESO and LA.

could deduce that only for temperatures above 80°C did a significant exotherm take place. This analysis is provided in Supporting Information from this article. On the other hand, the maximum temperature was deduced from TGA experiments. The weight loss (WL) as a function of the temperature for LA (Figure 9, shown later) revealed that above 100°C, the LA had a significant WL associated with LA boiling.

The volumetric standard methods ASTM 4274-99 and 1652-04 were applied to determine the OH number (OH#) and ring-opening yield (ROY) of the polyols. It was not possible to determine OH# at f_{LA} values lower than 0.25 because, during the procedure, the content in the flask turned dark brown, and the detection of the final point was not clear to the naked eye.

The IR absorption spectra of the polyols and their precursors were obtained with a MIRacle Single Reflection attenuated total reflection (ATR) accessory with a diamond prism in a Nicolet 480 FTIR spectrometer. We obtained each spectrum by recording 64 scans from 4000 to 525 cm^{-1} with a resolution of 4 cm^{-1}, whereas the Advanced ATR Correction facility of EZ Omnic software was used for their processing and correction with a theoretical refraction index of 1.5. The viscosities of the polyols were measured with a Brookfield digital viscometer (model DV-E) at 25°C. SEC was performed with a Waters instrument coupled with a refractive-index detector. Two Styragel columns (HR1 and HR4) were used consecutively, and tetrahydrofuran was used as the mobile phase with a flow rate of 1 mL/min. DSC was performed with a TA Q200 instrument with dynamic experiments. These consisted of three thermal steps: the first one, from –80°C to 250°C at a scan rate of 10°C/min; a second one, from 250 to –80°C at 10°C/min; and finally, a third one identical to the first. TGA was performed with a Shimadzu TGA 50 under a nitrogen atmosphere with a platinum crucible. Dynamic thermal analysis, which started at room temperature and went up to 800°C at a constant rate of 10°C/min, was applied.

DMA was carried out with a PerkinElmer DMA 8000 equipped with a liquid recirculation cooling system. The flexural mode was used, with the oscillation frequency fixed to 1.0 Hz and the amplitude to 0.01 mm. The thermal scan started at 5°C and went up to 180°C at a constant scan rate of 2°C/min. The samples had dimensions of 8 mm width by 20 mm length and 2 mm thickness. To reach such dimensions, the samples were cut with a Struers cutting machine (Minitom). Three repetitions for each formulation were tested. Before the sample was tested, its weight and dimensions were measured. It was corroborated that the experiments fell in the linear viscoelastic region of the material.

RESULTS AND DISCUSSION

Parametric Analysis of the ROY and OH# as a Function of the Temperature and f_{LA}

Parametric studies on how the ROY and the OH# were affected by the temperature and f_{LA} are depicted in Figures 2 and 3. As it is shown in Figure 2, ROY increased as a function of f_{LA}. For f_{LA}

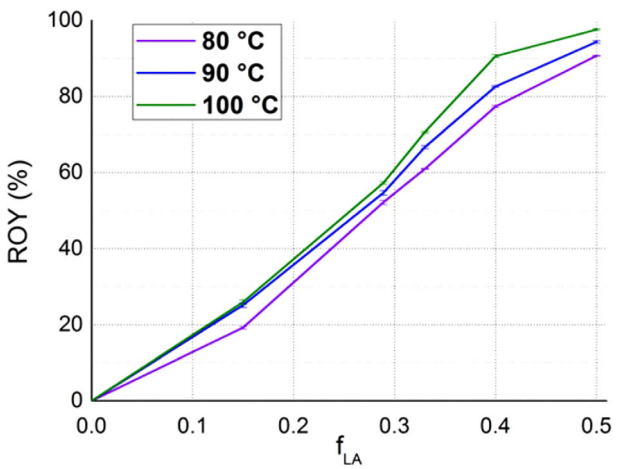

Figure 2. ROY as a function of f_{LA} and the temperature.

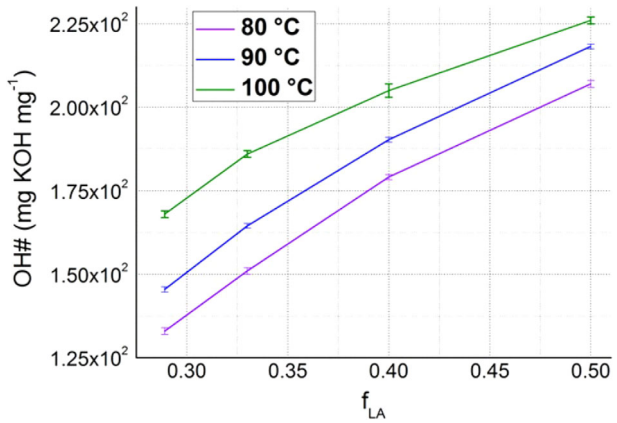

Figure 3. OH# as a function of f_{LA} and the reaction temperature.

values below 0.3, the slope of this graph was mostly independent of the temperature. However, for f_{LA} values above approximately 0.3, the slope was more dependent on the reaction temperature. Within this range, a higher reaction temperature was associated with a higher ROY.

The results depicted in Figure 2 are the first reported in the literature that encompass the dependency of ROY with f_{LA} and the reaction temperature. Even though other researchers have directly selected specific f_{LA} and reaction temperature values to perform ROR with LA,[42–44] it is imperative to perform this parametric analysis beforehand to achieve the optimum reaction conditions. The most relevant deduction from Figure 2 was that ROY was more dependent on f_{LA} than on the reaction temperature. Then, we observed that to achieve high ROY values, f_{LA} needed to be above 0.4, regardless of the reaction temperature. A simple expla-nation of this result can be introduced on the basis of the fact that two reactions were taking place, ROR by LA and oligomeri-zation. When higher f_{LA} values were used, from a chemical kinetic point of view, the overall reaction favored ROR by LA. On the other hand, for lower f_{LA} values, oligomerization pre-vailed. With respect to the temperature, at lower f_{LA} values, an increase in the temperature did not significantly change ROY because there was not enough LA reactant to overcome the oligo-merization kinetics. On the other hand, for higher f_{LA} values, ROR by LA prevailed; then, the temperature certainly had an effect on the final ROY because ROR by LA was more dependent on temperature. This gave rise to a lower oligomerization yield.

Once the reaction started, LA was not the only ROA. Although we weren't able to unravel the mechanism of oligomerization, it is possible to assert that a secondary reaction occurred, and the oxirane rings were opened either by LA (with the use of both functional groups) or by a hydroxyl group recently formed in the chain. Thus, a competition existed between at least two paths, and oligomers were formed.

ROY depended on both f_{LA} and the temperature, although the former was more determinant. The explanation for that situation is that f_{LA} represented the availability of LA to react with oxirane rings, whereas the temperature affected the reaction rate, more specifically, the reaction rate constant. As we already mentioned, more than one path to ring opening existed; however, an increase in the LA proportion caused ROY to rise significantly because more LA was able to react with the oxirane rings. That is, oligomerization occurred, but it could not complete the reaction itself, and higher amounts of LA were required to increase ROY. With respect to the temperature, an increase provoked the reaction rate constants to rise, either for ring opening by LA or oligomerization, but a slight difference favoring the former existed because the oligomeric content was lower at higher temperatures. Finally, according to the Arrhenius equation, the kinetic constant had a logarithmic dependence on the temperature, and a change from 80 to 90 or 100°C was not as important as the changes in f_{LA} that we carried out.

In the particular case of oligomerization, when f_{LA} and temperature increased, these secondary reactions become less competitive against ring opening by LA for all of the reactions mentioned in the last paragraph. Consequently, the polyol with the lowest oligomer content was the one prepared at the highest f_{LA} and temperature.

With respect to the OH# (Figure 3), it presented a monotonous increase for f_{LA} values starting at 0.25 and all of the way up to 0.5. The effect of the temperature on the OH# was associated with a higher absolute OH#. In other words, for any f_{LA} value, a higher temperature implied a higher OH#. However, this increase was also dependent on f_{LA}, whereas for higher f_{LA} values, the relative increase in the OH# as a function of the temperature was also reduced. The OH# for polyols ESO-P80, ESO-P90, and ESO-P100 were 174, 190, and 205 mg of KOH/mg, respectively, and they were free of residual acid.

The results depicted in Figure 3 are also the first reported in the literature that analyze the relationship between the OH#, f_{LA}, and reaction temperature. For certain specific values, the data followed what was found in previous studies.[43,44] Caillol *et al.*[43] reported a polyol prepared at 80°C with an OH# of 171 mg of KOH/mg, whereas Li and Sun[44] reported an OH# of 218.7 mg of KOH/mg for a reaction temperature of 90°C. The main deduction from Figure 3 is that the OH# was highly sensitive to both f_{LA} and the reaction temperature. Relatively small changes in both f_{LA} and the reaction temperature were associated with a change in OH#. This was particularly relevant for f_{LA} values below 0.4, in which the deviation of the OH# as a function of the reaction temperature had a higher spread. As a matter of fact, at the lowest f_{LA}, the maximum OH# spread was 26.1%, whereas at the highest f_{LA}, the spread was reduced to 9.1%.

Taking into account the results of Figure 3, we deduced that the maximum OH# of polyols obtained from ROR with LA were limited to what has been reported by Caillol *et al.*[43] These results might imply that the application of soybean polyols to rPUFs might be limited. This is because the OH# of polyester polyols frequently used in those formulations is usually above 300 or 400 mg of KOH/mg. Nonetheless, the polyester polyols had much lower F_{OH} values than the soybean polyols reported in this study. Then, it has to be emphasized that even though soybean-oil-based polyols might have lower OH# values, the possibility of attaining higher F_{OH} values will compensate for the decrease in the crosslinking density. In fact, Li *et al.*[44] reported the formation of a high-T_g network with such soybean polyols. Further discussion about F_{OH} is given later.

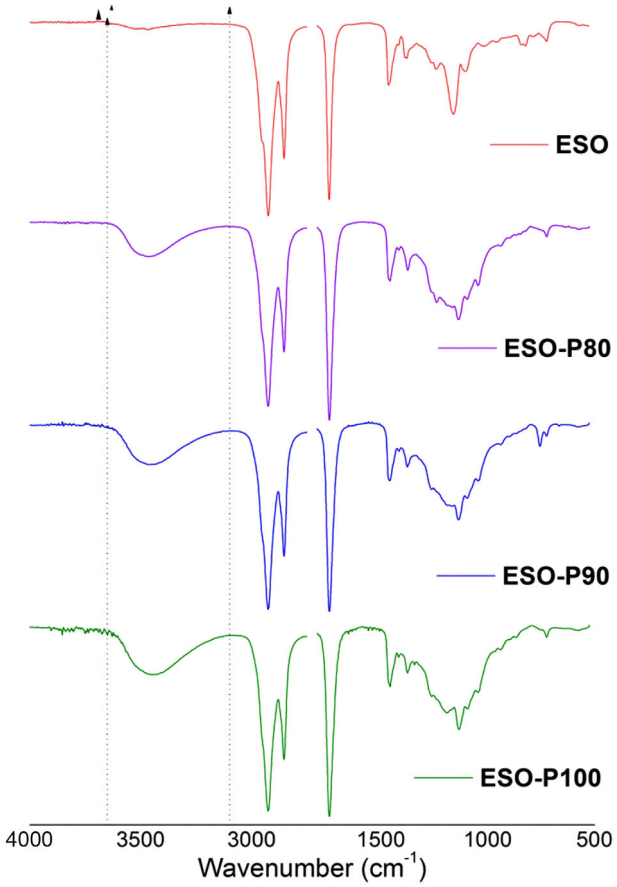

Figure 4. IR transmittance spectra of ESO, ESO–P80, ESO–P90, and ESO–P100.

FTIR Absorption and Transmittance Spectroscopy of the ESO–LA Polyols

ESO and polyols prepared at isothermal temperatures of 80°C (ESO-P80), 90°C (ESO-P90) and 100°C (ESO-P100), were analyzed by FTIR spectroscopy, and their spectra were registered in both transmittance and absorbance modes. In the transmittance spectra (Figure 4), it was possible to discern bands associated with the vibrational modes of several functional groups, for instance, ester C⌧O (1740 cm^{-1}), stretching (2925 and 2854 cm^{-1}) and bending (1463 and 1384 cm^{-1}) of alkane C—H, ester and ether C—O (1336–1050 cm^{-1}), hydroxyl (a band comprised in the region between 3650 and 3100 cm^{-1}), and oxirane (centered at 822.5 cm^{-1}).[45] These last two were the most interesting according to our purposes of analyzing the ROR and subsequent hydroxyl functionalization. As shown in Figure 4, the OH stretching band increased in its intensity and width in the order ESO < ESO–P80 < ESO–P90 < ESO–P100. This result was in agreement with what was theoretically expected. On the other hand, the study of the evolution of the oxirane absorption band is highlighted in Figure 5. The oxirane band absorption area presented a considerable reduction in the order ESO > ESO–P80 > ESO–P90 > ESO–P100. Furthermore, in the case of ESO–P100, the absorption band was almost negligible. Such a result also supports the hypothesis that the desired functionalization was achieved. In a comparison of the results presented with the ROY and the OH# analysis previously discussed, we deduced that the FTIR analysis corroborated the conclusions of the ROR analysis.

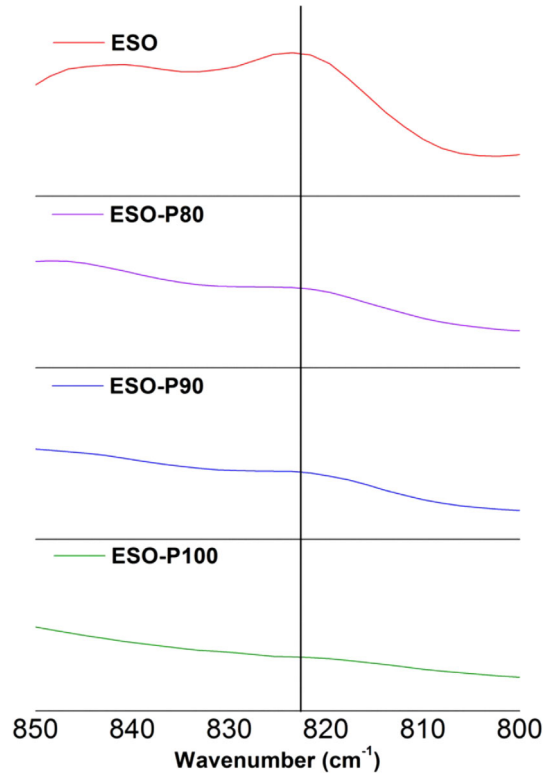

Figure 5. IR absorption spectra of the oxirane bands of ESO, ESO–P80, ESO–P90, and ESO–P100.

SEC of the ESO–LA Polyols

The results of the chromatographic analysis of ESO, ESO–P80, ESO–P90, and ESO–P100 are shown in Figure 6 for an f_{LA} value of 0.4 and Table I for all of the rest f_{LA} values. This figure depicts the weight percentage of monomers and oligomers obtained from the relative areas of the chromatographic peaks presented as a

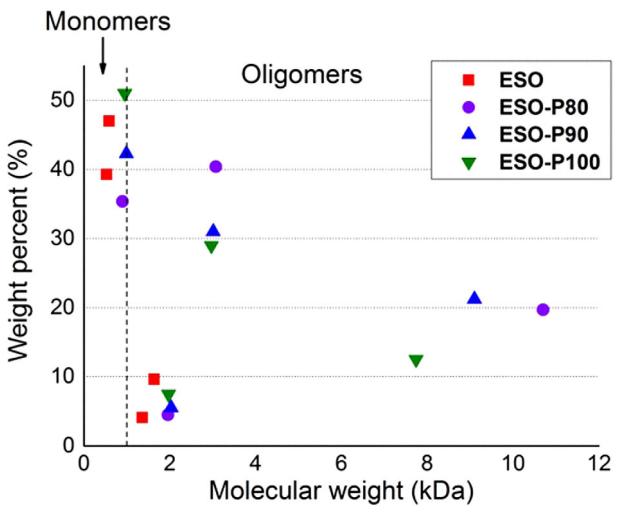

Figure 6. Weight distribution as a function of the molecular weight for ESO, ESO–P80, ESO–P90, and ESO–P100.

Table I. Physicochemical Properties of ESO, ESO–P80, ESO–P90, and ESO–P100 as a Function of f_{LA}

	f_{LA}	OH# (mg of KOH/g)	M_w (Da)	P_d	F_{OH}	Viscosity (Pa s)	Oligomeric content (wt %)
ESO	—	N.M.	696.6	1.14	2.9	0.325	13.7
ESO-P80	0.286	133	3332	1.60	7.90	N.M.	64.4
ESO-P90	0.286	145	3476	1.66	9.00	N.M.	59.85
ESO-P100	0.286	168	4219	1.85	12.6	N.M.	55.25
ESO-P80	0.33	151	4101	1.83	11.0	N.M.	63.4
ESO-P90	0.33	164	2915	1.36	8.52	N.M.	58.2
ESO-P100	0.33	185	2996	1.55	9.90	N.M.	49.1
ESO-P80	0.4	174	3754	2.13	12.0	42.2	64.6
ESO-P90	0.4	190	3392	1.97	11.5	39.0	57.7
ESO-P100	0.4	205	2462	1.69	9.0	36.3	49.0
ESO-P80	0.5	207	3366	1.5	12.4	N.M.	51.0
ESO-P90	0.5	218	2506	1.2	9.74	N.M.	44.9
ESO-P100	0.5	226	2326	1.31	9.37	N.M.	36.3

N.M., not measured.

function of molecular weight. As we noticed, ESO was composed mainly of monomers with molecular weights of 0.53 kDa (39.3 wt %) and 0.59 kDa (47 wt %); this represented 86.3% of the total weight. The different molecular weights of those monomeric species were due to the fact that soybean oil is not a unique triglyceride but a polydispersed mixture.[46] Despite the high purity of ESO, oligomers above 1 kDa accounted for 13.7 wt %. Considering that the epoxidation was based on the Prileshajev method, it was logical to obtain such a result. This was because the *in situ* formed peracetic acid formed a strong acidic environment, and this could lead to dimeric and trimeric species.[47–50]

For ESO–P80, ESO–P90, and ESO–P100 (all at f_{LA} = 0.4), the monomer content was significantly lower than for pure ESO. However, the specific monomer content was also highly dependent on the reaction temperature. In fact, higher temperatures favored the formation of an increased monomer content, from 35.4 wt % for ESO–P80 all the way up to 51 wt % for ESO–P100. This result indicated that at higher temperatures, the reaction of LA with the monomeric species of ESO was preferential in contrast to LA oligomerization. The major oligomeric component was the one with a molecular weight of around 3 kDa, presumably a trimer, and the oligomeric species with the highest molecular weight seemed to be composed of at least six monomeric units (even 9 or 10 in the case of the polyol ESO–P80) according to their molecular weights. The largest oligomers in ESO–P80, ESO–P90, and ESO–P100 had 11/12, 9, and 8 monomeric units, respectively, whereas their monomeric contents were 35.4, 42.3, and 51 wt %, respectively.

With respect to the oligomers, it was important to notice that for ESO–P80, ESO–P90, and ESO–P100 (all at f_{LA} = 0.4), the weight contents were considerable and well above the 13.7 wt % found in ESO. This was a clear indication that at least two competing reactions took place. One reaction was associated with the ROR of the ESO monomer with LA, and another one was associated with oligomerization. In this last case, several hypothetical reactions could have occurred, for example, interchain reactions among the ESO triglycerides, interchain reactions among the ESO triglycerides with LA as a bridge, or ROR caused by the R—COOH functionality of the LA.[42] Another important result was associated with the fact that the oligomeric weight content decreased as a function of an increased reaction temperature. For ESO–P80, it was 64.6 wt %; for ESO–P90, it was 57.7 wt %; and finally, for ESO–P100, it was 49 wt %. This tendency also explained why, at higher temperatures, the ESO–LA polymer was more monodispersed. In fact, when the temperature increased, the ROR by LA prevailed over ESO oligomerization.

In summary, there was a competition between ROR by LA and oligomerization that was dependent on the temperature. Although trimers were formed easily (they were the major oligomeric components in each polyol), the combination of small oligomers and the consequent formation of oligomers with higher monomeric units occurred predominantly at lower temperatures, whereas at higher temperatures, ring opening and the consequent formation of monomers was more important.

As we deduced from Table I and Figure 6, the reaction temperature interfered not only with the amount of oligomers but also with the weight-average molecular weight (M_w), polydispersity (P_d), and F_{OH}. M_w decreased by 34.4% after the reaction temperature was increased by only 20°C. Similarly, P_d was also reduced by 19%; this indicated that a higher reaction temperature implied a more monodisperse polymer. Finally, F_{OH} also decreased by 25%, going from 12.0 at a reaction temperature of 80°C all the way down to 9.0 for a reaction temperature of 100°C.

Another relevant aspect was the LA homopolymerization.[51] Several researchers performed reactions at temperatures considerably higher than 100°C, and none of them performed the reaction at 80, 90, or 100°C. For instance, Harshe *et al.*[52] carried out the polycondensation of LA at different temperatures with and without catalysts. The lowest temperature used in that study was 110°C, and the authors concluded than no homopolymerization was attained under those conditions. Moreover,

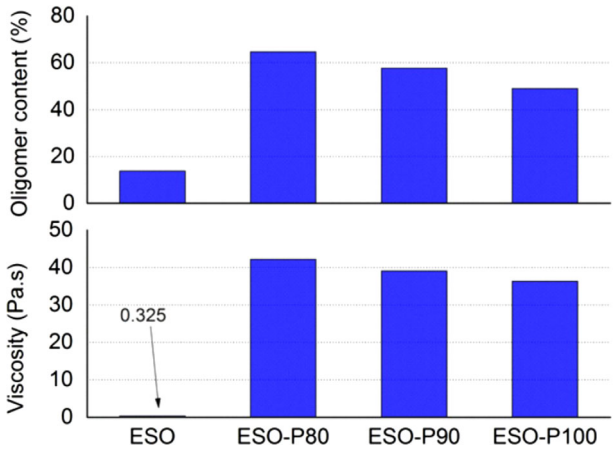

Figure 7. Comparison of the oligomeric content (weight percentage) and apparent viscosity as a function of the polyol type.

Li *et al.*[31] found similar results for reaction temperatures around 110°C.

These last results are useful for the development of polyols with tailored properties. For example, if a polyol with a higher functionality is needed, a lower reaction temperature can be used to achieve that purpose. This possibility is fundamental for polyols applied in rPUFs. As already mentioned previously, a highly functional polyol is preferable for achieving a highly crosslinked structure. This, in turn, will be translated in an rigid polyurethane foam (rPUF) with an improved thermomechanical performance and a higher T_g. Comparing our results with those from the literature, we ascertained that the polyols developed in this study had F_{OH} values that were more similar to what was found by Li *et al.*[44] Other researchers found F_{OH} values that were much lower than the ones reported here.[42,43] Another characteristic, which also conferred versatility, was that the reaction temperature also contributed to a change in the OH#. This, in turn, is also a desirable property that can be applied for the formulation of an rPUF. For example, a formulated polyol composed of 50 wt % ESO–P80 and 50 wt % ESO–P100 will give rise to an rPUF with a highly crosslinked nature and, simultaneously, a reduced friability. These last deductions emphasize that it is highly feasible to replace traditional polyols used in the rPUF industry with soy-based ones.

Apparent Viscosities of the ESO–LA Polyols

The apparent viscosities of ESO and the polyols were measured and compared to their oligomeric contents to establish a correla-tion between both experimental properties (Figure 7). At 25°C, the viscosity of ESO (0.325 Pa s) was considerably lower than those of the polyols. In addition, the viscosity was also dependent on the reaction temperature. A higher reaction temperature implied polyols with lower viscosities. For example, an increase in the reaction temperature from 80 to 100°C caused a decrease of 13.8% in the apparent viscosity. This result was also correlated with the reduction of the weight percentage of oligomeric species. As depicted in Figure 7, a reduction in the oligomeric content caused by an increase in the reaction temperature was also followed by a reduction in the apparent viscosity. Then, it was logical to deduce that the determination of the apparent viscosity could be used to estimate the oligomeric content.

As shown in Figure 7, there was a significant increase in the apparent viscosity between ESO and the polyols. Such an increase was coherent with the ROR used in this study, and it has also been reported by other researchers.[43,44] In fact, Li *et al.*[44] published a viscosity of 24.1 Pa s for a polyol having a OH# of 218.7 mg of KOH/mg, an F_{OH} of 11.7, and an M_w of 8800. On the other hand, Caillol *et al.*[43] reported a polyol with a viscosity of 47 Pa s, an OH# of 171 mg of KOH/mg, and an F_{OH} of 5.3. Our work was coherent with these results, and it also incorporated the dependence of the viscosity with the oligomeric content and, in turn, with the reaction conditions. In fact, as we mentioned before, a change in the reaction temperature was associated with a decrease in the viscosity. Such a result can be used for the development of soybean polyols, which could replace conventional polyester polyols. In fact, these last ones usually have a much lower functionality, ranging up to an F_{OH} of 5.0. Higher values of F_{OH} imply the formation of greases, which are much more difficult to incorporate into polyol formulations. In contrast, the polyols developed in this study had a very high F_{OH} and still a fairly low viscosity. In addition, the viscosity could be tailored by changing the reaction temperature. All of these aspects contribute to an increase in the versatility of soybean-oil-based polyols.

DSC of the ESO–LA Polyols

The thermal transitions of ESO, ESO–P80, ESO–P90, and ESO–P100 are depicted in Figure 8. In the case of ESO, a main transition associated with the melting and crystallization of different crystalline polymorphs was found from –40°C all the way up to –10°C. Such a transition has already been reported in other publications.[53,54] For the case of the polyols, such a transition was also measured, but it was dissociated into several transitions that covered a wider temperature range. In addition, the transitions shifted to higher temperatures with respect to ESO. For example, for ESO–P80, a transition was found centered at 8.0°C. Such

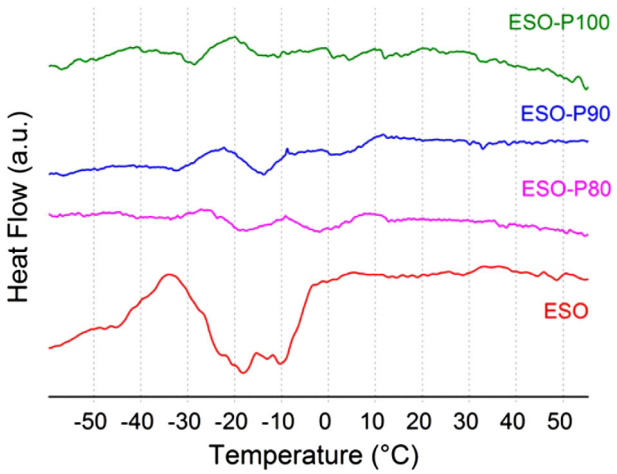

Figure 8. Thermal transitions of ESO, ESO–P80, ESO–P9, and ESO–P100.

observations were in agreement to what was found by Li *et al.*[44] Another relevant aspect was associated with the fact that for the polyols, the number of transitions was clearly reduced as a function of increasing reaction temperature.

We understood these results by taking into account the molecular structure of each polymer. For ESO, the fact that it had a very high content of monomeric species implied the formation of a preponderant thermal transition, which was studied before by several researchers.[53–55] On the other hand, the polyols presented a more polydispersive molecular structure; hence, it was logical to measure several thermal transitions associated with the nature of each oligomeric species. The fact that the transitions were observed at higher temperatures was expected because the additional hydroxyl groups incorporated by the LA functionalizations increased the intermolecular interactions of the molecular chains and increased the structural regularity. On the other hand, the area under the melting transitions clearly decreased for the polyols; this indicated a less compact crystal structure. In other words, it was logical to find that molecular chains with higher molecular weights formed isolated crystals, which were not as compact as the crystals of the ESO polyol.

We obtained a very relevant conclusion by comparing the results of the thermal transitions and the SEC analysis. As mentioned previously, an increase in the reaction temperature was followed by a decrease in the oligomeric content. Simultaneously, the number of thermal transitions was also reduced. This represented a logical correlation between the results obtained by DSC analysis and the SEC experiments. We attempted to compare the thermal transitions of the polyols obtained in this study with those of others reported in literature.[44] However, only one work dealt with this important aspect. It should be emphasized that future research should include these studies. One of the main applications of the polyols developed in this research area is rPUFs. The low-temperature behavior of rPUFs is strongly associated with the structure and crystallinity of the soft segment, which is defined by the polyol physicochemical structure.

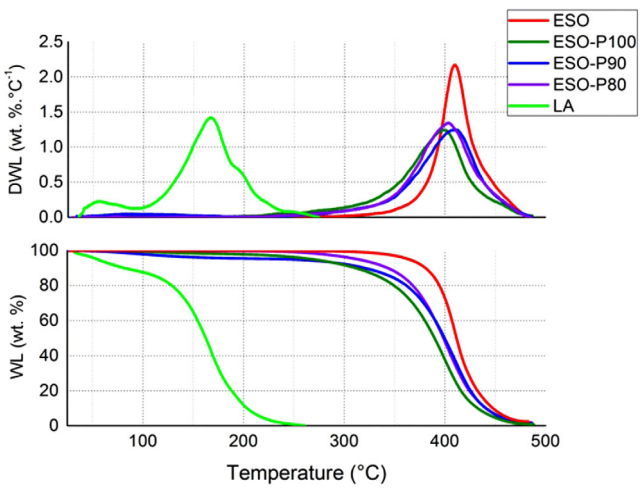

Figure 9. WL and DWL as a function of the temperature for ESO, ESO–P80, ESO–P90, and ESO–P100.

Table II. Formulation and Properties of the rPUFs Synthesized from ESO–LA

Component	pbW	Apparent density (kg/m^3)	Growth cell dimension (μm)
rPUF-ESOf_{LA1}-A			
Isocyanate	79.1	50.1 ± 1.9	
NCO index	105		
ESO-LA-P90-f_{LA1}	100		
H_2O	2		392 ± 55.1
Surfactant	2		
DBTDL	1		
rPUF-ESOf_{LA1}-B			
Isocyanate	112.4	34.3 ± 1.5	
NCO index	105		
ESO-LA-P90-f_{LA2}	100		
H_2O	4		314 ± 71.5
Surfactant	2		
DBTDL	1		
rPUF-ESOf_{LA2}-A			
Isocyanate	91.6	50.9 ±0.89	487 ± 90.1
ESO-LA-P90-f_{LA2}	100		
H_2O	2		
Surfactant	2		
DBTDL	1		
rPUF-ESOf_{LA2}-B			
Isocyanate	126.02	33.65 ± 3.8	397 ± 34.4
NCO index	105		
ESO-LA-P90-f_{LA2}	100		
H_2O	4		
Surfactant	2		
DBTDL	1		

pbW, parts by weight; DBTDL, dibutyltin dilaurate.

Thermogravimetric WLs of the ESO–LA Polyols

The WL and the differential weight loss (DWL) values as functions of the temperature for LA, ESO, ESO–P80, ESO–P90, and ESO–P100 are depicted in Figure 9.

The WL of LA consisted mainly of two stages. One covered the range 25–110°C, which implied a total WL of 13 wt % and had a maximum DWL centered at approximately 53°C. On the other hand, the second stage covered the range 110–260°C and implied a WL of roughly 87 wt %. The maximum DWL of this stage was centered at 167°C. From a previous study,[56] we inferred that the initial stage was associated with the evaporation of water and methanol impurities. On the other hand, the subsequent stage was indeed the thermal degradation of LA and lactide. These results highlight that there was a range in which the ROR reaction was feasible and that the temperature range should have been below 110°C. Any increase in the reaction temperature

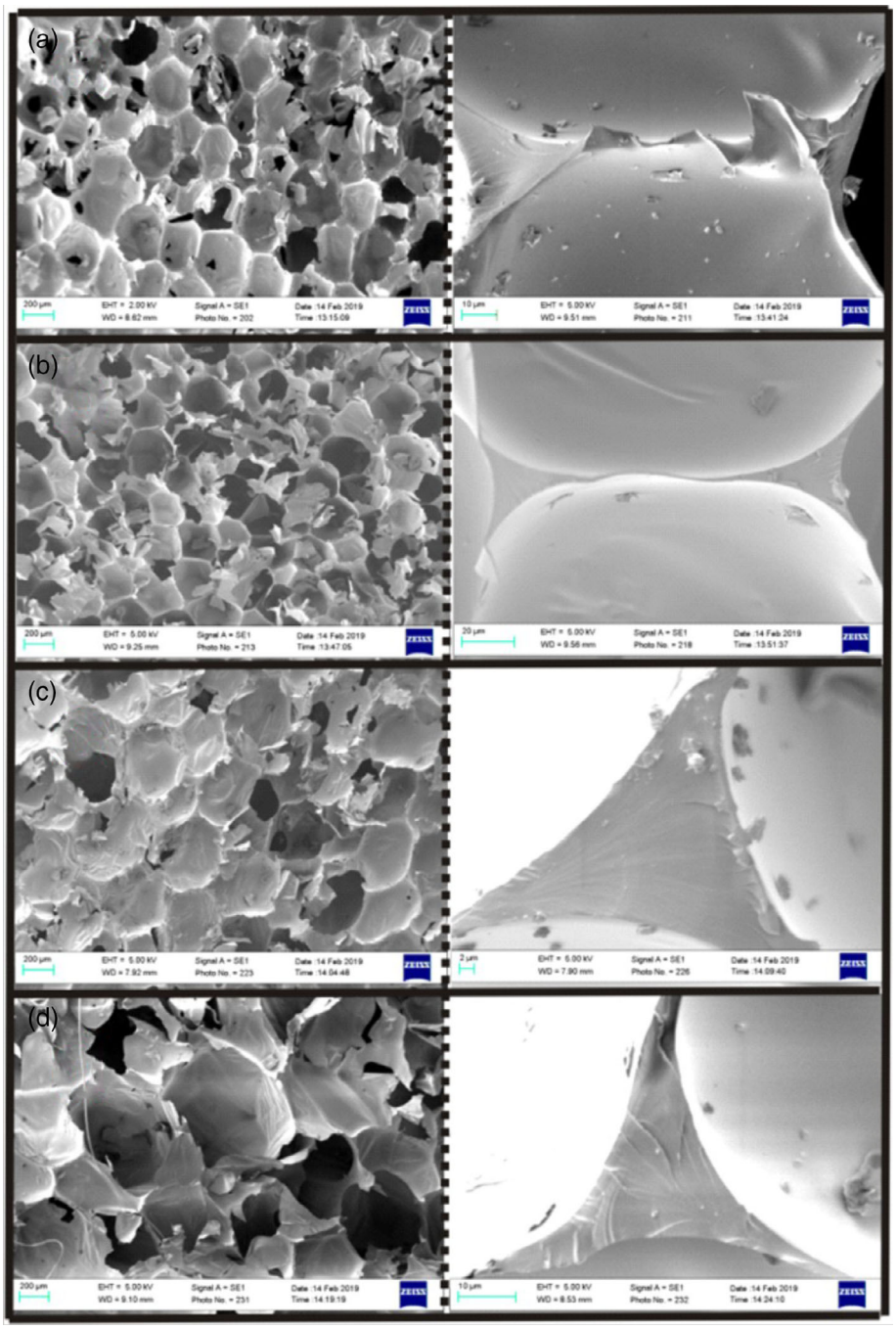

Figure 10. Scanning electron microscopy micrographs showing the cell (left column) and strut morphology for (a) rPUF–ESOf$_{LA1}$–A, (b) rPUF–ESOf$_{LA1}$–B,(c) rPUF–ESOf$_{LA2}$–A, and (d) rPUF–ESOf$_{LA2}$–B.

caused the boiling of LA and had an adverse effect on ROY and the OH# of the synthesized polyols. In other words, we believe that it was not possible to increase the reaction temperature to obtain higher values of ROY and OH# or to decrease the oligomeric content of the polyols because it would imply an undesired competition between ROR and LA decomposition.

The WL and DWL of ESO consisted mainly of a single stage, which started at temperatures above 300°C and went up to 500°C and left a residue of 2 wt %. The maximum DWL was centered at 410°C. As already noticed by other researchers,[43,44] a very good thermal stability can be achieved with ESO as a precursor.

For the case of the polyols (ESO–P80, ESO–P90, and ESO–P100), the WL and DWL consisted also of a central stage centered at relatively high temperatures, such as ESO. In contrast to ESO, the DWL of the polyols covered a wide temperature range. For example, for the case of ESO–P80, even at temperatures around 150°C, a small DWL was measured. In addition, the maximum DWL of the polyols was significantly lower with respect to the one of ESO. A slight shift to lower temperatures also indicated

that the polyols had a relatively lower thermal performance. Then, one of the drawbacks of using LA as an opening agent is that the resulting molecular structure has a lower thermal performance. However, this change is not considerable and can be disregarded for most applications.

rPUFs Based on the ESO–LA Biobased Polyols

The ESO–LA polyols were used to synthesize rPUFs based on the formulations depicted in Table II. As discussed, two variables were studied, polyol OH# and BA concentration. The rPUF–$ESOf_{LA1}$–A represented an rPUF based on an ESO reacted at an f_{LA} of 0.285 and at a reaction temperature of 90°C with a foaming agent concentration of 2 wt % (A is equivalent to this concentration). The rPUF–$ESOf_{LA2}$–B was synthesized via increases in f_{LA} (f_{LA2} = 0.4) and the foaming agent concentration (B is equivalent to 4 wt %) but with the maintenance of the reaction temperature at 90°C.

Apparent Densities and Cell Morphologies of the rPUFs

As can be deduced from Table II, for a fixed BA value, an increase in f_{LA} caused a negligible change in the apparent density; this indicated that the foaming reaction was not altered by the changes in OH# (or f_{LA}). In contrast, the apparent density changed considerably as a function of the BA concentration. An increase in BA from 2 to 4 wt % caused an average decrease in the apparent density of 31.6%. Such a variation was expected because BA was the primordial source of carbon dioxide during the synthesis of the foam. Hence, any change in BA certainly affected its apparent density. The electronic micrographs of the surface of the rPUFs developed in this study are depicted in Figure 10. The left column shows the shape and size of the cells, whereas the right column shows higher magnification micrographies and focuses on the geometry of the struts and cell walls. In a comparison of rPUFs prepared at a fixed OH# [Figure 10(a,b)], an increase in the BA concentration caused a reduction of the average cell size from 392 ± 55.1 to 314 ± 71.5 μm as well as a reduction in the apparent density. From these results, we deduced that the addition of water in the formulation caused an increase in the kinetics of formation of the polyurea linkage in contrast to polyurethane. Such hypothesis could also be deduced because the cell windows of rPUF–$ESOf_{LA1}$–B were more stable than the ones of rPUF–$ESOf_{LA1}$–A. This was a clear indication that even though the foam had a lower density, the strength of the cells was improved. A similar result was obtained with the rPUFs prepared with a lower polyol OH [Figure 10(c,d)]. On the other hand, in a comparison of the rPUF prepared at a fixed BA [Figure 10(a,c)], we deduced that a reduction in OH# caused a negligible change in the apparent density but an increase of 24.2% in the cell size (Table II). These results further enhanced the hypothesis that the kinetics of formation of the polyurethane linkages caused by the reaction of the isocyanate and the polyol were lower with respect to the formation of polyurea linkages, as noted before.

Compression Mechanical Tests and DMA of the rPUFs

The compressive stress as a function of deformation for rPUF as a function of BA and the f_{LA} value is depicted in Figure 11. For each configuration, the stress as a function of the deformation followed linear elastic, plateau, and densification regions.[57] If two rPUFs with identical BA concentrations were compared, we deduced that an increase in the OH# (or f_{LA}) was followed by an upward shift of the compressive stress versus deformation curve. Such a result was logical because a polyol with a higher OH# should have also been translated into a higher crosslinked structure and, hence, an improved compressive response. On the other hand, if two rPUFs were compared with an identical f_{LA}, we deduced that an increase in the BA concentration was followed by a downward shift in the compressive stress as a function of the deformation. This was another expected result because an increase in the BA concentration caused a reduction in the apparent density of the foam and, hence, a reduction in the compressive stress as a function of the deformation.

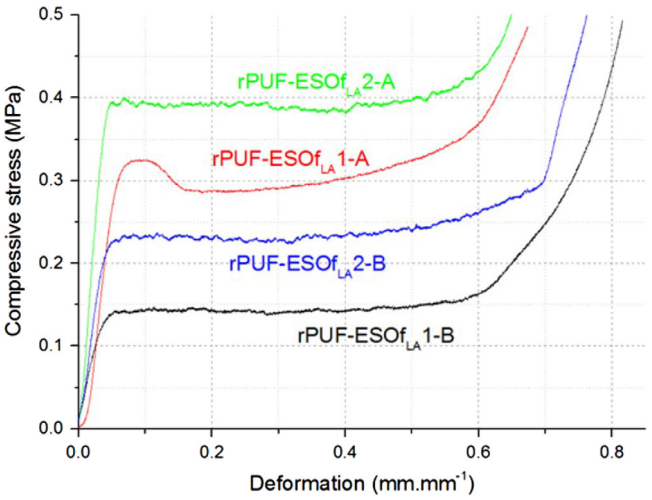

Figure 11. Compressive stress as a function of deformation for rPUFs synthesized from ESO–P90 at f_{LA} = 0.285 and f_{LA} = 0.4 with BA concentrations of 2 and 4 wt %.

To compare the results obtained in our study with what has already been published, as highlighted by Lobos and Velankar,[58] it is important to calculate the specific compressive strength. Using the values deduced from Figure 11 and Table II, we calculated that the specific compressive strengths of the rPUFs developed in this study fell within the range 4.37–7.8 kPa kg^{-1} m^3. The highest value was attained with the lowest BA concentration (2 wt %) and an f_{LA} value of 0.4. In contrast, the lowest value was measured for the highest BA concentration (4 wt %) and an f_{LA} value of 0.285. This result highlighted the relevance of F_{OH} with respect to the OH#. To attain the highest specific compressive strength, an increase in F_{OH} had a more relevant impact than an increase in OH#. Comparing our results with what has been found in literature, the highest specific value reported so far was ascribed to Tu *et al.*,[59] with a value of 7.2 kPa kg^{-1} m^3. Other values reported in the literature fell below this value, even though some formulations were also prepared with glycerin as a crosslinker or with blends of commercially available polyols.[60–71] Then, we deduced that the specific compressive strength obtained in our study was very high, even though no additional crosslinkers were added in the formulation.

The specific elastic modulus (E'_{sp}) and the damping factor (tan δ) as a function of the temperature for the rPUFs synthesized in this study are shown in Figure 12. At room temperature, the

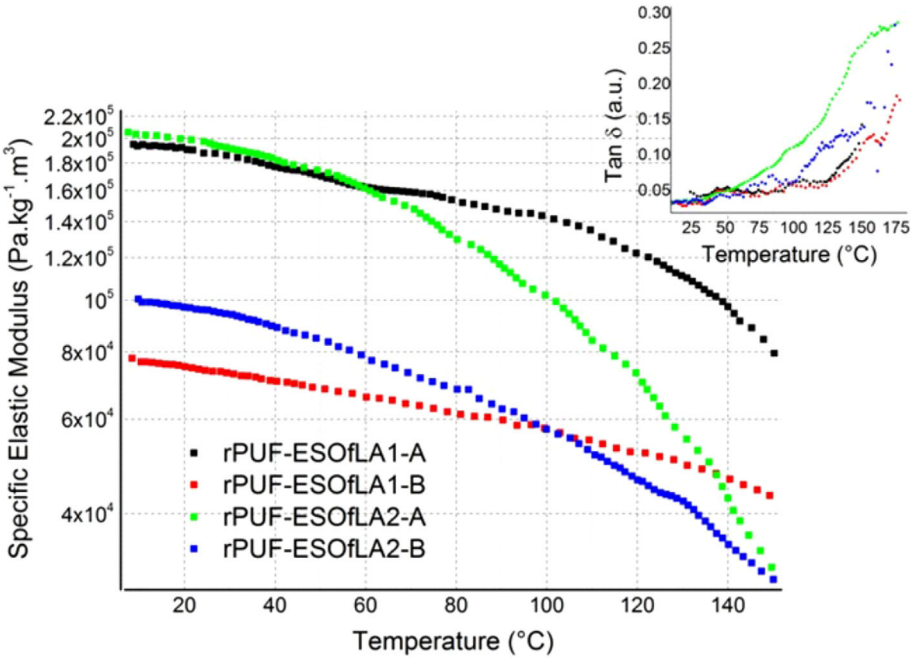

Figure 12. E'_{sp} and damping factor (inset) as a function of the temperature for rPUFs synthesized at $f_{LA2} = 0.4$ and $f_{LA1} = 0.28$ at a fixed temperature of 80°C at two different BA concentrations (A = 2 wt % and B = 4 wt %).

variation in E'_{sp} as a function of the BA concentration and polyol OH# showed a similar trend as the one found in the compressive mechanical tests explained previously. In fact, the highest E'_{sp} was found for the formulation with the lowest BA concentration (2 wt %) and an f_{LA} value of 0.4. On the other hand, the variation in E'_{sp} as a function of the temperature was mostly dependent on the f_{LA} value instead of the BA concentration. As a matter of fact, a higher f_{LA} value implied a steeper decrease in E'_{sp} as a function of the temperature; this gave the highest damping factor for an f_{LA} value of 0.4 and a BA concentration of 2 wt %. These results highlighted the fact that if rPUF is used for applications with temperatures above 60°C, it is better to use a formulation with a higher OH# to prevent a significant reduction in E'_{sp}. Then, we deduced that a compromised relationship arose between the specific compressive strength and the temperature dependence of such a property. To increase the first one, the most relevant aspect was to increase F_{OH}. Instead, to increase the latter one, the OH# had to be maximized. This was because of the presence of oligomeric species. Such species might not react completely with the isocyanate and may leave the material with a lower physical crosslinking density, as already noted.[17,29,72,73]

Future work will also consider the simulation of the effects of F_{OH}, oligomeric content, and OH# on the thermomechanical properties of rPUF with the constitutive models presented by Bodaghi *et al.*[73–75]

CONCLUSIONS

Biobased polyols were successfully synthesized from ESO with a nontoxic protocol based only on ESO and LA. A parametric analysis of the ROR of ESO with LA as a function of the temperature and f_{LA} revealed that it was possible to obtain polyols with a very high functionality (12.4) by performing experiments at lower temperatures (80°C) and high f_{LA} values (0.5). The physicochemical properties of the polyols were mainly associated with the competition of ROR by LA and oligomerization. At lower f_{LA} values, oligomerization prevailed, whereas at higher f_{LA} values, ROR by LA prevailed. The effect of the reaction temperature had a more profound effect at higher f_{LA} values, where ROR by LA prevailed.

rPUFs based solely on the polyols developed in this study were synthesized, and we obtained very high specific compressive strength values (7.8 kPa kg^{-1} m^3) for polyols synthesized with an F_{OH} value of 12.4. These results emphasize that formulations based solely on soy-based polyols have the potential to replace conventional petroleum-derived polyester polyols applied in rPUFs. DMA revealed a compromised relationship of E'_{sp} as a function of the temperature. If it is important to achieve the highest specific compressive modulus at ambient temperature, it is necessary to maximize F_{OH}. Instead, if the objective is to have an rPUF with a wider temperature stability, the OH# has to be maximized.

Further work in this area should focus on the reduction in the viscosity of the soybean polyol with the maintenance of a high OH# and F_{OH}. Another relevant aspect is an increase in the reaction rates, which serve for the development of a scalable soybean polyol.

ACKNOWLEDGMENTS

The authors thank Marcelo Nestor Stola from Varteco for kindly providing ESO and Matías Nonna from Huntsman Argentina. This work was supported by the *Agencia Nacional de Promoción Científica y Tecnológica* (Argentina) through PICT 2015 N0475. The authors also extend their appreciation to Adrián Bartomioli and Rocío Tognetti for providing their artwork.

REFERENCES

1. Mosiewicki, M. A.; Aranguren, M. I. *Polym. Int.* **2016**, *65*, 28.

2. Mosiewicki, M. A.; Aranguren, M. I. *Eur. Polym. J.* **2013**, *49*, 1243.
3. Thakur, V. K.; Thakur, M. K.; Kessler, M. R. Handbook of Composites from Renewable Materials: Polymeric Composites; Wiley: Hoboken, NJ, **2017**.
4. Puglia, D.; Sarasini, F.; Santulli, C.; Kenny, J. M. Green Biocomposites; Springer: New York, **2017**.
5. Fortunati, E.; Yang, W.; Luzi, F.; Kenny, J.; Torre, L.; Puglia, D. *Eur. Polym. J.* **2016**, *80*, 295.
6. Peponi, L.; Puglia, D.; Torre, L.; Valentini, L.; Kenny, J. M. *Mater. Sci. Eng. Rep.* **2014**, *85*, 1.
7. Tschan, M. J.-L.; Brulé, E.; Haquette, P.; Thomas, C. M. *Polym. Chem.* **2012**, *3*, 836.
8. Frollini, E.; Rodrigues, B. V.; da Silva, C. G.; Castro, D. O.; Ramires, E. C.; de Oliveira, F.; Santos, R. P. AIP Conf. Proc. 2016, 427, 020033.
9. Lligadas, G.; Ronda, J. C.; Galià, M.; Cádiz, V. *Biomacromolecules*. **2010**, *11*, 2825.
10. Meier, M. A.; Metzger, J. O.; Schubert, U. S. *Chem. Soc. Rev.* **2007**, *36*, 1788.
11. de Oliveira, F.; Ramires, E. C.; Frollini, E.; Belgacem, M. N. *Ind. Crops Prod.* **2015**, *72*, 77.
12. Ramires, E. C.; de Oliveira, F.; Frollini, E. *J. Appl. Polym. Sci.* **2013**, *129*, 2224.
13. Panda, S.; Mohanty, P.; Behera, D.; Kumar Bastia, T. *J. Appl. Polym. Sci.* **2016**, *133*, 44345. https://doi.org/10.1002/app.44345
14. Mashouf Roudsari, G.; Misra, M.; Mohanty, A. K. *J. Appl. Polym. Sci.* **2017**, 134.
15. Petrović, Z. S.; Zlatanić, A.; Lava, C. C.; Sinadinović-Fišer, S. *Eur. J. Lipid Sci. Technol.* **2002**, *104*, 293.
16. Cui, S.; Luo, X.; Li, Y. *Int. J. Adhes. Adhes.* **2017**, *79*, 67.
17. Cordero, A. I.; Amalvy, J. I.; Fortunati, E.; Kenny, J. M.; Chiacchiarelli, L. M. *Carbohydr. Polym.* **2015**, *134*, 110.
18. Kirpluks, M.; Kalnbunde, D.; Benes, H.; Cabulis, U. *Ind. Crops Prod.* **2018**, *122*, 627.
19. Prociak, A.; Kurańska, M.; Cabulis, U.; Ryszkowska, J.; Leszczyńska, M.; Uram, K.; Kirpluks, M. *Ind. Crops Prod.* **2018**, *120*, 262.
20. Ng, W. S.; Lee, C. S.; Chuah, C. H.; Cheng, S.-F. *Ind. Crops Prod.* **2017**, *97*, 65.
21. Septevani, A. A.; Evans, D. A. C.; Annamalai, P. K.; Martin, D. *J. Ind. Crops Prod.* **2017**, *107*, 114.
22. Zhang, K.; Hong, Y.; Wang, N.; Wang, Y. *J. Appl. Polym. Sci.* **2018**, *135*, 45779.
23. Alagi, P.; Ghorpade, R.; Jang, J. H.; Patil, C.; Jirimali, H.; Gite, V.; Hong, S. C. *Ind. Crops Prod.* **2018**, *113*, 249.
24. Da, L.; Gong, M.; Chen, A.; Zhang, Y.; Huang, Y.; Guo, Z.; Li, S.; Li-Ling, J.; Zhang, L.; Xie, H. *Acta Biomater.* **2017**, *59*, 45.
25. Chiacchiarelli, L. Biomass, Biopolymer-Based Materials, and Bioenergy; Elsevier: Amsterdam, **2019**.
26. Randall, D.; Lee, S. The Polyurethanes Book; Wiley: Hoboken, NJ, **2003**.
27. Szycher, M. Szycher Handbook of Polyurethanes; Taylor & Francis: Boca Raton, FL, **2013**.
28. Cheng, M.-H.; Rosentrater, K. A. *Ind. Crops Prod.* **2017**, *108*, 775.
29. Gimenez, R. B.; Leonardi, L.; Cerrutti, P.; Amalvy, J.; Chiacchiarelli, L. M. *J. Appl. Polym. Sci.* **2017**, *134*.
30. Li, Y.; Luo, X.; Hu, S. Bio-Based Polyols and Polyurethanes; Springer: New York, **2015**.
31. Li, Y.; Wang, D.; Sun, X. S. *RSC Adv.* **2015**, *5*, 27256.
32. Mosiewicki, M.; Casado, U.; Marcovich, N.; Aranguren, M. *Polym. Eng. Sci.* **2009**, *49*, 685.
33. Chen, R.; Zhang, C.; Kessler, M. R. *J. Appl. Polym. Sci.* **2015**, 132.
34. Miao, S.; Zhang, S.; Su, Z.; Wang, P. *J. Appl. Polym. Sci.* **2013**, *127*, 1929.
35. Omrani, I.; Farhadian, A.; Babanejad, N.; Shendi, H. K.; Ahmadi, A.; Nabid, M. R. *Eur. Polym. J.* **2016**, *82*, 220.
36. Bouriazos, A.; Vasiliou, C.; Tsichla, A.; Papadogianakis, G. *Catal. Today*. **2015**, *247*, 20.
37. Dumont, M.-J.; Kharraz, E.; Qi, H. *Ind. Crops Prod.* **2013**, *49*, 830.
38. Kandanarachchi, P.; Guo, A.; Petrović, Z. *J. Mol. Catal. A*. **2002**, *184*, 65.
39. Cabrera Munguia, D. A.; Tzompantzi, F.; Gutiérrez-Alejandre, A.; Rico, J. L.; González, H. *Energy Proceed.* **2017**, *142*, 582.
40. Prociak, A.; Malewska, E.; Kurańska, M.; Bąk, S.; Budny, P. *Ind. Crops Prod.* **2018**, *115*, 69.
41. Komesu, A.; Martinez, M.; Fazzio, P.; Lunelli, B. H.; Oliveira, J.; Wolf Maciel, M. R.; Maciel Filho, R. *J. Chem.* **2017**, 2017.
42. Miao, S.; Zhang, S.; Su, Z.; Wang, P. *J. Polym. Sci. Part A: Polym. Chem.* **2010**, *48*, 243.
43. Caillol, S.; Desroches, M.; Boutevin, G.; Loubat, C.; Auvergne, R.; Boutevin, B. *Eur. J. Lipid Sci. Technol.* **2012**, *114*, 1447.
44. Li, Y.; Sun, X. S. *Int. J. Adhes. Adhes.* **2015**, *63*, 1.
45. Radojcic, D.; Ionescu, M.; Petrović, Z. S. *Contemp. Mater.* **2013**, *4*, 9.
46. Dorni, C.; Sharma, P.; Saikia, G.; Longvah, T. *Food Chem.* **2018**, *238*, 9.
47. Gen Klaas, M. R.; Warwel, S. *J. Am. Oil Chem. Soc.* **1996**, *73*, 1453.
48. Sinadinović-Fišer, S.; Janković, M.; Petrović, Z. S. *J. Am. Oil Chem. Soc.* **2001**, *78*, 725.
49. Cai, C.; Dai, H.; Chen, R.; Su, C.; Xu, X.; Zhang, S.; Yang, L. *Eur. J. Lipid Sci. Technol.* **2008**, *110*, 341.
50. Warwel, S. *Ind. Crops Prod.* **1999**, *9*, 125.
51. Greco, A.; Ferrari, F.; Maffezzoli, A. *J. Therm. Anal. Calorim.* **2018**, *134*, 559.
52. Harshe, Y. M.; Storti, G.; Morbidelli, M.; Gelosa, S.; Moscatelli, D. *Macromol. React. Eng.* **2007**, *1*, 611.

53. Guo, A.; Cho, Y.; Petrović, Z. S. *J. Polym. Sci. Part A: Polym. Chem.* **2000**, *38*, 3900.
54. Dai, H.; Yang, L.; Lin, B.; Wang, C.; Shi, G. *J. Am. Oil Chem. Soc.* **2009**, *86*, 261.
55. Buffa, J. M.; Mondragon, G.; Corcuera, M. A.; Eceiza, A.; Mucci, V.; Aranguren, M. I. *Eur. Polym. J.* **2018**, *98*, 116.
56. Komesu, A.; Martins Martinez, P. F.; Lunelli, B.; Hoss, N.; Oliveira, J.; Wolf Maciel, M. R.; Maciel Filho, R. *J. Chem. 2017*, **2017**, 7.
57. Avalle, M.; Belingardi, G.; Montanini, R. *Int. J. Impact Eng.* **2001**, *25*, 455.
58. Lobos, J.; Velankar, S. J. *Cell. Plast.* **2016**, *52*, 57.
59. Tu, Y. C.; Kiatsimkul, P.; Suppes, G.; Hsieh, F. H. *J. Appl. Polym. Sci.* **2007**, *105*, 453.
60. Tan, S.; Abraham, T.; Ference, D.; Macosko, C. W. *Polymer*. **2011**, *52*, 2840.
61. Guo, A.; Javni, I.; Petrović, Z. *J. Appl. Polym. Sci.* **2000**, *77*, 467.
62. Hu, S.; Wan, C.; Li, Y. *Bioresour. Technol.* **2012**, *103*, 227.
63. Veronese, V. B.; Menger, R. K.; Forte, M. M. D. C.; Petzhold, C. L. *J. Appl. Polym. Sci.* **2011**, *120*, 530.
64. Guo, A.; Zhang, W.; Petrović, Z. S. *J. Mater. Sci.* **2006**, *41*, 4914.
65. Javni, I.; Zhang, W.; Petrović, Z. *J. Polym. Environ.* **2004**, *12*, 123.
66. Tu, Y. C.; Suppes, G. J.; Hsieh, F. H. *J. Appl. Polym. Sci.* **2008**, *109*, 537.
67. Guo, A.; Demydov, D.; Zhang, W.; Petrović, Z. S. *J. Polym. Environ.* **2002**, *10*, 49.
68. Fan, H.; Tekeei, A.; Suppes, G. J.; Hsieh, F. H. *J. Appl. Polym. Sci.* **2013**, *127*, 1623.
69. Gu, R.; Konar, S.; Sain, M. *J. Am. Oil Chem. Soc.* **2012**, *89*, 2103.
70. Ji, D.; Fang, Z.; He, W.; Luo, Z.; Jiang, X.; Wang, T.; Guo, K. *Ind. Crops Prod.* **2015**, *74*, 76.
71. Campanella, A.; Bonnaillie, L.; Wool, R. *J. Appl. Polym. Sci.* **2009**, *112*, 2567.
72. Kenny, J. M.; Torre, L.; Chiacchiarelli, L. M. *J. Appl. Polym. Sci.* **2015**, 132.
73. Bodaghi, M.; Damanpack, A.; Liao, W. *Smart Mater. Struct.* **2018**, *27*, 065010.
74. Bodaghi, M.; Damanpack, A.; Liao, W. *Smart Mater. Struct.* **2016**, *25*, 105034.
75. Bodaghi, M.; Damanpack, A.; Liao, W. *Mater. Des.* **2017**, *135*, 26.